DESIGN OF A BEAM HALO MONITOR WITH A HIGH DYNAMIC RANGE

J. Egberts[1], S. Artikova[1], E. Bravin[2], T.Chapman[3], T. Lefèvre[2], M.Pilon[3], C.P. Welsch[1,4,5]
[1]MPI-K, Heidelberg, [4]University of Heidelberg, [5]GSI, Darmstadt, Germany
[2]CERN, Geneva, Switzerland,[3]Thermo Fisher Scientific, Liverpool, NY USA

Abstract

A thorough understanding of halo formation and its possible control is highly desirable for essentially all particle accelerators. Limiting the number of particles in the halo region of a beam would allow for minimizing beam losses and maximizing beam transmission, i.e. the experimental output. Measurements based on either optical transition radiation (OTR) or synchrotron radiation (SR) provide an interesting opportunity for high dynamic range measurements of the transverse beam profile, since the signal is linear with the beam charge over a wide range and is routinely used in many diagnostic applications. In this contribution, first results on beam halo measurements obtained from a flexible core masking technique and an innovative CID camera system are summarized.

INTRODUCTION

The detection and possible control of the beam halo is of utmost importance for high energy accelerators, where unwanted particle losses lead to an activation or even damage of the surrounding vacuum chamber [1], [2]. But also in low-energy machines, like the ultra-low energy storage ring (USR) [3] at the future facility for antiproton and ion research (FLAIR) [4], one is interested in minimizing the number of particles in the tail region of the beam distribution. Since most part of the beam is normally concentrated in the central region, observation techniques with a high dynamic range are required to ensure that halo particles can be monitored with sufficient accuracy. One option to monitor the beam halo is to use light generated by the beam, either through SR, OTR, or luminescent screens. In thus case, a special camera technology is required to allow for high dynamic range measurements.

But also for low energy accelerators and storage rings like the USR such measurements can be envisaged by e.g. exploiting the light from a phosphor screen.

In order to approximate a typical beam distribution as it is found in an accelerator we used a conventional laser beam in our lab. The open angle of the laser of 0.1 corresponds to SR/OTR emitted at some 100 MeV and can be regarded as a realistic approximation of a real particle beam.

CID CAMERA

The charge injection device (CID) derives its name from its unique ability to clear individual pixel sites of photon-generated charge by injecting the charge directly into the substrate. The main features of this imager technology are its distinctive readout capabilities including inherent resistance to ionizing radiation, inherent resistance to charge blooming, true random pixel addressability, non-destructive pixel readout (NDRO), and on-sensor collective pixel readout and clear.

Architecture

The on-sensor collective read feature allows the data acquisition routines to select contiguous pixel regions (e.g., a 3 by 3 pixel region) and interrogate those pixels with a single reading that is the electronic average of the signals on those pixels, thereby improving both readout speed and signal-to-noise ratio. This collective read feature is analogous to the binning that can be performed with certain CCD camera systems. However, unlike the CCD where the charge packets from the individual pixels are physically combined into a single larger charge packet, the CID collective read feature preserves the spatial integrity of the photon-generated charge in the pixels and the read process is non-destructive to that charge. The CID architecture also allows for the clearing of photon-generated charge from contiguous pixel regions with a single inject pulse. Similar to most micro-electronic devices built today, the CID is manufactured with silicon technology. A single crystal silicon wafer forms the substrate of the device. The insulating Si substrate is doped with boron to make it electrically conductive (p-type). Upon the substrate, an n-doped epitaxial layer is grown. As the thickness of the epitaxial layer is increased, the full well capacity and NIR response also increase. The epitaxial layer is slightly doped in such a manner as to cause minority signal carrier diffusion into the bulk silicon. Next, a thick field oxide is grown in a checker board pattern across the surface of the wafer. The field oxide is an isolating layer, a dielectric film, composed of silicon dioxide. A thin gate oxide of about 400 nm of SiO_2, is grown over the remaining exposed epitaxial layer. Conductive poly-silicon is then applied in thin strips that regularly crisscross the entire surface of the imager forming the row and column electrodes. The two orthogonal poly-silicon electrodes are electrically isolated and connect pixels to the processing electronics at the periphery of the device. One electrode is designated the column or sense electrode and the other is the row or drive electrode. The region at the intersection of the two electrodes under the thin gate oxide delineates the active charge-storage area for each pixel.

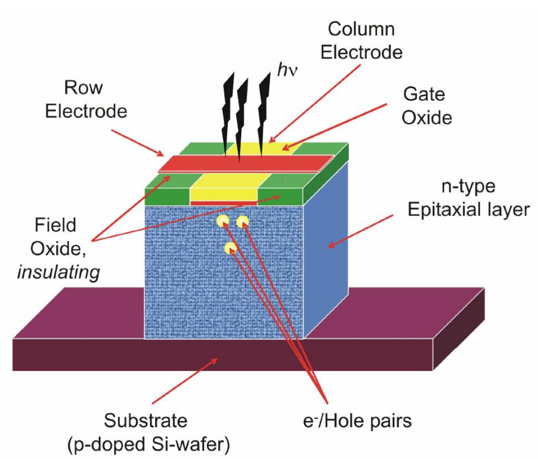

Figure 1: Layout CID pixel.

Readout

Each pixel on the CID imager is individually addressable and allows for random access non-destructive pixel readout.

During charge generation, the row electrode is set on a high and the column electrode on a low potential. Since the photon generated charge is collected in the form of positively charged holes, the charge will pile up underneath the column electrode. The potential of the row electrode is measured and the column electrode is then set to an even lower voltage, which causes the holes to migrate toward the row electrode. When charge moves in or out of a capacitor, the electrode potential will change according to $dV = dQ/C$. Therefore, the change of the sense electrode potential is proportional to the amount of accumulated charge. After the readout of the pixel, the electrodes can either be set to their original potentials or the holes can be injected into the substrate layer where they will recombine with the electrons. The non-destructive pixel readout (NDRO) is one of the unique features of the CID camera [5].

Once the charge within a pixel exceeds a certain threshold value, the pixel can be read and thereby emptied independently from the others. Highly illuminated pixels will be emptied more often often than just slightly illuminated ones. Especially for very long exposure times, the number of readouts is a good mass for the light intensity. The ”Extreme Dynamic Range” (XDR) algorithm provided by the ”SpectraCam Racid Exposure” [6] software takes full advantage of this unique feature of the CID-camera and thereby maximises the achievable dynamic range [7].

Since the dark current would normally have a negative effect on the accumulated charges for long exposure times and low light intensities, the pixel array is down to -37°C by a thermoelectric cooling device. The heat is then transferred by water tubes to an external chiller. The dynamic range is therefore mainly limited by the readout frequency on the one hand, and the maximum acceptable light intensity on the other.

System Callibration

In order to callibrate the camera system, a setup with a well-defined light source was used. It consists of the OSL1-EC [8] and a fibre illuminator with an adjustable light output of up to 100 W. At the end of the light guide, a little box with several diffusors was mounted to generate a homogeneous light distribution.

Behind the diffusors, a mask with different neutral density filters was attached. The homogeneous light that passes through the filters thus obtains a well-known intensity. By measuring the light transmission for various neutral density filters and light intensities, the specifications of the camera can be determined.

Measuring a Laser Profile

Since the light intensity of the laser is too high for the CID-camera to handle, it was reduced by a neutral density filter. The laser beam profile was then obtained by directing the laser beam directly onto the pixel array without any objective lenses in between.

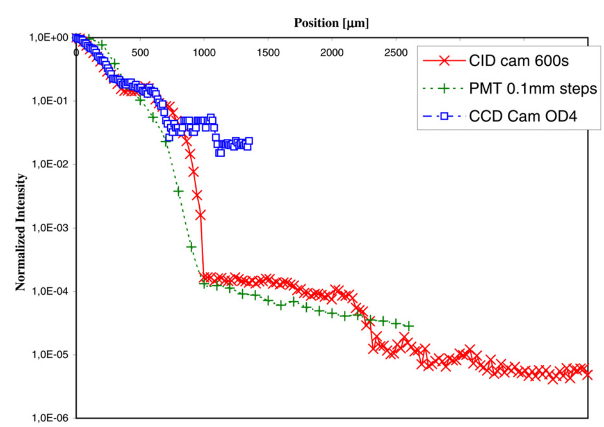

Figure 2: Beam profile of CCD (blue), CID (red) and PMT (green) [5].

In fig. 2 the normalised beam profile is shown as it was acquired by a CCD-camera (blue), a CID-camera (red) and a photomultiplier tube (green). By covering five orders of magnitude, the CID-camera grants the highest dynamic range combined with a high spatial resolution. Since it is possible to save the data in an ASCII-file, the data can be analysed by a C++ program which fits a Gaussian function to the data, determines the standard deviation σ, and on this basis, defines the beam halo as the amount of light outside of $n\sigma$.

MASKING OUT THE BEAM CORE

Another option to measure the beam halo is to mask out the main beam core. If the intense light from the beam core is blanked out, a normal camera can monitor the halo without saturation and overexposure. An example of earlier measurements at CERN is given in fig. 3. In the first picture, a beam profile is shown through a 10% neural density filter, in the second, the beam core is masked out, and in the third, the neutral density filter is removed [9]. Again, one can clearly see the halo after the removal of the neutral density filter. Nevertheless, in contrast to the measurement with the CID-camera, this method does not grant a direct comparison between the halo and the beam core. On the other hand, it does not require the high dynamic range of a CID-camera but a normal 8 bit CCD-camera can be used. This yields the advantage of far lower costs for the camera and the option of an online beam halo monitoring since the large exposure time of the CID-camera is not required.

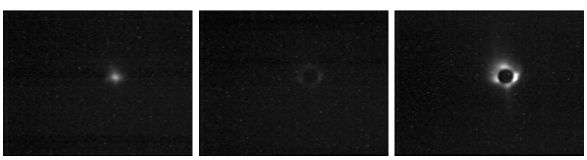

Figure 3: Masking out the beam core [9].

Micro Mirror Array

A strong limitation in the first tests with the core masking technique was the fixed shape of the mask itself. For time dependent beam profile measurements a technique is required to generate a mask based on (online) measurements of the beam. In our setup, we realize a flexible mask by using a Micro-Mirror-Array (MMA).

An MMA consists of an array of 1024×768 micro mirrors of $13.68\mu\text{m}\times13.68\mu\text{m}$ size which can be tilted by 12° in two directions. Each micro mirror can be steered individually and therefore the MMA can be used to display arbitrary shapes. If the beam core profile is displayed on the MMA and illuminated by the laser beam, the main beam core is deflected in another direction than the beam halo.

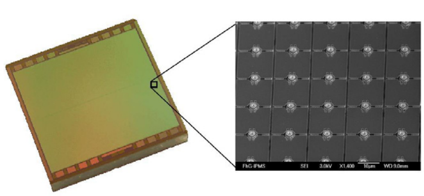

Figure 4: MMA with Enlargement of pixel structure[10].

A careful callibration of the overall optics is required to ensure that a pixel as measured by the camera system can be mapped on an MMA pixel. The correct adjustment of the image of the beam core on the MMA display is of critical importance. If the beam core does not fit to its image on the MMA, the MMA will not be able to properly mask out the beam core which will lead to an overexposure of the camera. Since the spatial resolution of the MMA and the CID-camera is in the micrometer regime, it is desirable to achieve an adjustment of laser, camera and MMA with comparable precision. In addition, the interference pattern generated by the MMA needs to be carefully investigated.

Outlook

The Spectracam XDR is a next-generation CID camera which promises extreme dynamic ranges and will be tested in our optical laboratory within the next few months.

In contrast to this high-end camera technology, the Micro Mirror Array provides a relatively simple solution to generate spatially highly variable masks on very short time scales.

After successful tests in the lab, beam tests with both devices are foreseen which will allow for a direct comparison of the performances.

REFERENCES

[1] E. Guignard et al, "A 3TeV e+ e- Linear Collider Based on the CLIC Technology", CERN-2000-008

[2] R. Schmidt et al, "Beam loss scenarios and strategies for machine protection at the LHC", Proc. 3rd HALO ICFA Advanced Beam Dynamic Workshop, Montauk, USA (2003)

[3] C.P. Welsch, M. Grieser, J. Ullrich, A. Wolf, "An ultra-low-energy storage ring at FLAIR", Nucl. Instr. Meth. A 546 (2005) 405417

[4] C.P. Welsch, H. Danared, "FLAIR: A Facility for Low-energy Antiproton and Ion Research", Proc. Europ. Part. Acc. Conf., Edinburgh, Scotland (2006)

[5] C.P. Welsch, E. Bravin, B. Burel, T. Chapman, T. Lefvre, M.J. Pilon, "Alternative Techniques for Beam Halo Measurements", Meas. Sci. Technol. 17 (2006) 2035c, CERN-AB-2006-23

[6] Thermo Scientific, http://www.thermo.com

[7] M.J. Pilon, private communication

[8] Thorlabs, Inc., http://www.thorlabs.com

[9] T.Lefèvre, H.Braun, E. Bravin, R. Corsini, D. Schulte, A. L. Perrot, "Beam Halo Monitoring at CTF3", Proc. EPAC, Lucerne, Switzerland (2004)

[10] Bakke, T., Völker, B., Friedrichs, M., Rudloff, D., "Micromirror Array of Monocrystalline Silicon", International Conference on Optical MEMS and their Applications 2006, pp: 128-129